LBL-15874
c.2

Lawrence Berkeley Laboratory
UNIVERSITY OF CALIFORNIA

RECEIVED
BERKELEY LABORATORY

MAY 16 1983

LIBRARY AND
DOCUMENTS SECTION

Presented at the Sixth Oaxtepec Symposium,
Institute of Physics of the University of Mexico,
Mexico City, Mexico, January 4-7, 1983

THE ONSET OF INCOMPLETE MOMENTUM TRANSFER IN FUSION-LIKE PROCESSES

R.G. Stokstad, Y. Chan, M. Murphy, I. Tserruya,
S. Wald, and A. Budzanowski

March 1983

Prepared for the U.S. Department of Energy under Contract DE-AC03-76SF00098

LBL-15874
c.2

DISCLAIMER

This document was prepared as an account of work sponsored by the United States Government. While this document is believed to contain correct information, neither the United States Government nor any agency thereof, nor the Regents of the University of California, nor any of their employees, makes any warranty, express or implied, or assumes any legal responsibility for the accuracy, completeness, or usefulness of any information, apparatus, product, or process disclosed, or represents that its use would not infringe privately owned rights. Reference herein to any specific commercial product, process, or service by its trade name, trademark, manufacturer, or otherwise, does not necessarily constitute or imply its endorsement, recommendation, or favoring by the United States Government or any agency thereof, or the Regents of the University of California. The views and opinions of authors expressed herein do not necessarily state or reflect those of the United States Government or any agency thereof or the Regents of the University of California.

LBL-15874

The Onset of Incomplete Momentum Transfer in Fusion-like Processes.

R. G. Stokstad, Y. Chan, M. Murphy, I. Tserruya, and S. Wald

Lawrence Berkeley Laboratory
University of California
Berkeley, CA 94720

and

A. Budzanowski
Institute of Nuclear Physics
Cracow, Poland

Invited talk presented by R. G. Stokstad at the sixth Oaxtepec Symposium sponsored by the Institute of Physics of the University of Mexico, January, 1983.

ABSTRACT

Velocity spectra of evaporation residues from the reactions ^{16}O + Al, Ca, and Ni have been measured at bombarding energies of 8.8, 13.6, and 19.6 MeV/u. Comparison with statistical model predictions shows clear evidence for the onset of incomplete momentum transfer at about 5 MeV/u above the interaction barrier. To first order, the results are similar for all targets, suggesting that the missing momentum is mainly associated with the projectile. The fraction of transferred linear momentum appears to decrease linearly with increasing relative velocity of the colliding nuclei at the barrier.

I. Introduction.

There is a rich vocabulary associated with the study of heavy-ion reaction mechanisms. Authors develop new and picturesque terms to describe the results of their most recent experiments. Different-sounding names may refer to the same physical process, and the same expression might be used occasionally to refer to totally different physical phenomena. When in doubt, the prefix "quasi" can be (and is) attached to just about anything. Depending on whether one is a critic or advocate of the field, one might take the above as a sign of imprecision and confusion or, as I would prefer, of vitality and discovery. In any case, it is essential to define one's terms as precisely as possible; I will try to do this, hoping that those of you thoroughly familiar with the jargon will be patient.

Suppose two nuclei are brought together with no excess kinetic energy at the point of contact. If the attractive nuclear forces are greater than the repulsive Coulomb forces, then the nuclei will most likely swallow each other and form a compound nucleus which reaches equilibrium. It is very unlikely that, e.g., one half of the projectile would be captured and the other half repelled. Thus, at low bombarding energies, fusion dominates the reaction cross section. In this process, all of the projectile is captured and, therefore, all of the momentum is transferred from the projectile to the compound system. The attainment of equilibrium implies that particles are emitted subsequently and in any direction with equal likelihood (with modifications imposed by angular momentum

conservation). To be specific, this process, including the requirement of equilibrium, is called complete fusion.

It is clear that at bombarding energies well in excess of the interaction barrier and characteristic nuclear potential energies, the above process will be small or nonexistent; the nucleons in the projectile are simply moving too fast for all of them to be captured and thermalized with any significant probability. What actually happens will depend on many variables, such as bombarding energy, masses of the projectile and target, impact parameter and so on. One possibility is that a portion of the projectile may fuse with the target while the remainder proceeds much as a spectator. Clearly this process will depend on the overlap of projectile and target and, therefore, on the impact parameter. If one starts at zero impact parameter, where one assumes (for discussion) that complete fusion occurs, the emergence of the above phenomenon is naturally called incomplete fusion.[1] If, on the other hand, one begins with a grazing collision, where inelastic scattering and few-nucleon transfer reactions dominate, and progressively decreases the impact parameter, the term "massive transfer" is suggested.[2] These terms are both used in the literature and refer to the same mechanism. More generally, the term pre-equilibrium emission has been used for many years in association with light-ion induced reactions.[3]

It is interesting to study this mechanism because it falls between two extremes, because it reflects the balance of competing forces, and because it may contain information on the time scale of

the reaction. There is abundant experimental evidence that these processes occur for heavier targets, and strong indications for lighter targets as well.[4-6]

In this particular case, the starting point is complete fusion. Because fusion reactions have been studied for many years, there is both empirical knowledge of, and theoretical foundation for, the signatures of this process. The mass, velocity, and excitation energy of the compound nucleus are known. One has, in addition, clues to the range of angular momenta involved from the size of the measured fusion cross section. (The usual assumption is that fusion occurrs for all ℓ for which $\ell \leq \ell_c$ and

$$\sigma_{fus} = \pi \lambda\!\!\!^{-2} (\ell_c + 1)^2$$

The statistical model (with empirical input parameters) predicts the decay of the compound nucleus. Thus, the signature of incomplete fusion or any nonequilibrium process is a departure from the predictions for complete fusion.

Evidence for these processes may be found in the characteristics of (i) the light particles (p,n,d,α) which are emitted at forward angles, (ii) the fragments of the projectile that did not fuse with the target, or (iii) the heavy residue left behind. In general, inclusive measurements of a light particle or a projectile-like fragment are insufficient to establish the mechanism. A two-particle coincidence involving, e.g., a characteristic gamma ray from the heavy residue[1,2] is required. However, observation of a heavy particle with a mass and velocity

near to that expected for a compound nucleus specifies that a reaction approximating fusion (fusion-like) took place. The idea is thus very simple. Measure the velocities of the residues and compare them with what is expected for complete fusion. If they are smaller than expected, we may infer that a nonequilibrium process was involved, and that it caused an incomplete transfer of momentum from the projectile to the target. Measurements as a function of bombarding energy will determine the threshold. While the basic idea may be simple, a number of important complications are encountered both in doing the experiment and interpreting the results. These will be dealt with in the following sections.

II. The Experiment.

The 88-Inch Cyclotron at Lawrence Berkeley Laboratory can produce beams of oxygen ions with energies of up to 20 MeV/nucleon. These energies are high enough that nonequilibrium processes should be easy to see. The targets, Al, Ca, and ^{60}Ni, were chosen with the following criteria: (i) The targets should be significantly heavier than the projectile. This is necessary for a clear interpretation of the reaction kinematics.[+] (ii) The target should be light enough to produce residues with sufficiently high energy to be detected easily. Very heavy targets fission and thus require a different technique for measuring momentum transfer.[7]

[+]To illustrate this point, consider identical projectile and target nuclei; in this case, incomplete capture of one object by the other would occur with equal probability for target and projectile. There would be no net shift of the average residue velocity. The width of the velocity distribution would be broader, however.

The masses and velocities of the residues were measured with the time-of-flight spectrometer illustrated schematically in Fig. 1. The start signal was obtained from a channel-plate detector with a thin carbon conversion foil, about 20 $\mu gm/cm^2$, tilted at an angle of 45° to the 1.8 meter long flight path. The stop detector, a 900 mm^2, 100 μm thick silicon surface-barrier detector, was tilted by 15° to the flight path in order to minimize geometrical path differences. The stop detector also determined the energy of the residues. The targets were natural calcium, natural aluminum, and ^{60}Ni with thicknesses of 235, 215 and 180 $\mu gm/cm^2$, respectively.

An essential part of this experiment was to establish an accurate absolute calibration for the velocity. This was done by measuring the elastic scattering of 1.5 MeV/nucleon ^{40}Ar ions, which have masses and velocities similar to those of the residual nuclei produced in the reactions studied. This calibration procedure is illustrated in Fig. 2, where the velocities and flight times of ^{40}Ar and ^{16}O ions, elastically scattered by a variety of targets at several different scattering angles, are indicated. The calibration covers nearly all the range of velocities observed in the experiments. Corrections (typically a few percent) for energy loss in the target and in the carbon foil of the start detector were made in the calibration procedure and, event-by-event, in generating the final velocity spectra.

The mass resolution is indicated in Figs. 3 and 4. Fragments with masses of less than 20 were not necessarily stopped within the depletion depth of the detector. This accounts for the truncation

of the spectra at the lighter masses. Figure 4, a projection onto the mass axis of the two-dimensional spectrum in Fig. 3, also gives an idea of the relative mass yields. The presence of a group of evaporation residues is clear in both these figures.

A typical velocity spectrum for a given mass is shown in Fig. 5. For reasons which will be given in a moment, the ordinate is the number of counts divided by the square of the measured velocity. Note that the distribution is broad and well approximated by a Gaussian. The breadth of this spectrum is one of the complications I mentioned earlier. Relatively light ($A < 100$) compound nuclei emit copious amounts of charged particles when they deexcite. Alpha particle emission is frequent and the resulting recoil imparted to the residue is significant. It is not possible to measure, therefore, the velocity of an <u>individual</u> compound nucleus prior to the evaporation stage.

If, however, the decay process is symmetric about 90° in the center-of-mass system of the emitting nucleus, then the centroid of the velocity distribution of all residues observed at 0° should be the same as that of the original compound nucleus. This statement is true provided the distribution plotted is $N(v)/v^2$ and not $N(v)$.[8] (Note that the Lorantz-invariant cross section, $\frac{1}{p}\frac{d^2\sigma}{d\Omega dE}$, is proportional to $\frac{1}{v^2}\frac{d^2\sigma}{d\Omega d\bar{v}}$.) There is an additional correction factor of $\cos\theta$, where θ is the laboratory angle at which the residues are detected. Thus, it can be shown that the centroid $\bar{v}$ of the distribution $N(v)/v^2$ is given by $v_{c.m.}\cos\theta$, where $v_{c.m.}$ is the velocity of the center-of-mass motion.

The only assumptions are full momentum transfer and symmetric forward-backward emission of subsequent light particles. If, in addition, the emission is isotropic, then $N(v)/v^2$ should have a Gaussian shape.[8]

This simple treatment also suggests that the centroid of the velocity spectrum should be independent of the number of particles emitted and, hence, independent of the mass of the residue. This is shown in Figs. 6 and 7, where velocity spectra are shown for different residue masses observed at a given laboratory angle and produced at three different bombarding energies. Note that the experimental centroid changes little with mass and that the width of the distribution correlates well with the difference Δ in mass between compound and residue nucleus, $\Delta = 56-A$.

III. Results.

The results of the experiment consist of the velocity spectra measured for each mass (or mass bin) at several laboratory angles between 5° and 20°, ^{16}O beams of 8.8, 13.6 and 19.6 MeV/nucleon, and targets of ^{27}Al, ^{40}Ca, and ^{60}Ni. The results obtained with the different targets were qualitatively similar; thus, data for $^{16}O + {}^{40}Ca$ will be used for illustrating the results. In principle, all the above information - velocity, mass, and angular distributions - may be compared with the predictions for complete fusion. For the present, we have concentrated on a comparison of the centroids with $v_{c.m.}\cos\theta$. This comparison is

given in Figs. 8-11. The first three of these figures give the centroid, measured at different angles, as a function of residue mass. The centroids were determined both by direct numerical evaluation and by fitting a Gaussian function to the data. These two methods agreed to within about 3%. The relative mass yields are indicated.

Several features are immediately obvious in Figs. 8-10.

(i) The centroids vary only weakly with residual mass.

(ii) The centroids scale with angle as $\cos\theta$.

(iii) The deviation of the experimental centroid from $v_{c.m.}\cos\theta$ varies only weakly with angle.

The discrepancy between the experimental centroid and the expectation for full momentum transfer is indicated in Fig. 11 for the three bombarding energies. The deviations, averaged over all masses, are 6%, 11% and 20% for bombarding energies of 8.8, 13.6 and 19.6 MeV/nucleon, respectively. The errors in the experimental centroids are typically 5-8% and arise from uncertainties in the velocity calibration, the centroid determination, and the corrections for energy loss in the target. Thus the difference from the predicted values is well outside experimental error, especially for the higher bombarding energies.

IV. Discussion.

The first step is to verify the accuracy of the simple prediction, $v_{c.m.}\cos\theta$, for the centroid. This was done by using the Monte Carlo code LILITA[8,9] to simulate the decay of ^{56}Ni

formed in the ^{16}O + ^{40}Ca reaction. The centroids from the simulation calculation agreed very well with $v_{c.m.}\cos\theta$. Thus, the measurement of the centroid of the residue velocity distribution is a measure of the average velocity of the compound system before it decays by equilibrium emission and therefore, of the average momentum transfer.

An assessment of the size or importance of the deviations indicated in Fig. 11 can be made as follows. Suppose, just for illustration, that a particle of mass Δm escapes at 0° with the beam velocity before fusion and equilibration occur. Then the deviations of 6%, 11% and 20% correspond to Δm = 0.9, 2.1 and 3.8 mass units, respectively, Thus, a deviation of 6% could be caused by a neutron or proton escaping in 90% of all collisions, or an alpha particle escaping in 60% of all collisions. In terms of the percentage of all collisions experiencing some degree of incomplete momentum transfer (i.e., between 90% and 60%), a six percent velocity shift is already a large effect!

The purpose of the present experiments is to investigate the dependence of the missing momentum on the projectile energy and target mass. For this we shall use the observed angle and mass-averaged velocity centroids expressed as a percentage of the velocity corresponding to full momeuntum transfer. This quantity is plotted in Fig. 12 versus the relative velocity of the colliding partners at the interaction barrier (using r_o = 1.5 fm). Although there is some dispersion in the data, an apparent systematics emerges. First, the amount of transferred momentum, expressed

as a percentage of the total available linear momentum, is governed essentially by the relative velocity of the projectile and target at the barrier. Second, there is no marked target dependence, at least over the range from A = 27 to A = 60. The absence of a target dependence suggests that the missing momentum is associated with the ^{16}O projectile.

The data also exhibit approximately linear behaviour in the decrease of the fraction of transferred momentum as a function of velocity, as indicated by the straight-line fit to the data. A similar result has been reported by Viola et al.[10] for reactions involving ^{12}C, ^{16}O and ^{20}Ne beams with the targets Au and U. For comparison, the results of linear momentum transfer measurements using ^{16}O projectiles and a ^{238}U target[7] are also indicated in Fig. 12. These results suggest a common onset of incomplete momentum transfer in fusion-like reactions at about 5 MeV/nucleon above the interaction barrier.

The questions of systematic behavior raised in Fig. 12 can be addressed further by the inclusion of results for other projectiles. The other beams that can be fairly included in this comparison are, at present, ^{12}C and ^{20}Ne. In one case[11] $^{20}Ne + {}^{40}Ca$, the experimental technique and analysis were the same as in our work. In most of the other cases, the fission-fragment angular-correlation method was used. Duek et al. have made new measurements and have reanalyzed earlier data using this technique.[12] In order to be included in Fig. 13, there should be an identifiable fusion-like component for which a centroid may be

determined. If the very small momentum transfer components resulting from one- and two-nucleon transfer reactions are merged with the fusion-like component in the determination of the centroid, the comparison of the different results breaks down. Similarly, the data are restricted to cases with a significant projectile-target mass asymmetry.

The data points shown in Fig. 13 may be identified with the aid of Table I. Note that the range of projectile masses is 12 to 20, target masses, 27-238, and bombarding energies, 6.2-30 MeV/nucleon. The reader will have to judge the extent of systematic behavior. There is additional scatter associated with the inclusion of additional measurements, of course. Different experimental techniques are involved, and no attempt has been made to evaluate the errors assigned by the different authors. We would suggest that a gross systematics is present. The assessment of individual deviations from the average behavior and their significance will have to await more precise experiments.

A simple systematic behavior (if verified) suggests a simple reaction mechanism. The idea that incomplete fusion is governed by a critical angular momentum (which varies with the captured mass and the radius of the target) has been put forward by Siwek-Wilczynska et al.[1] A detailed comparison of our results for $^{16}O + ^{40}Ca$ with this model will be given in the future. However, we may note that their model (with input parameters as given in Ref. 1) underestimates the observed shift in the velocity centroid. (In this comparison, only captured masses from ^{8}Be to ^{16}O were

included, and the missing mass was assumed to proceed at 0° with the beam velocity.) A comparison of predicted and observed systematic trends for different projectile-target combinations is in progress.

An important question which present and future experiments should resolve is whether the emission mechanism depends on a critical angular momentum (and therefore on the product of mass, velocity and radius) or on the penetration of a wall (the surface of the nucleus) by the nucleons. In the latter case, the essential quantities would be relative velocity and binding energy. Much is known about projectile fragmentation, and the capture of one portion of a projectile that fragments at an early stage of the collision has also been considered.[13]

On the experimental side there are a number of things which have to be done. The test of projectile dependence must be expanded to include beams other than the α-conjugate family. Measurements with ^{14}N and ^{19}F are desirable. Finally, coincidence experiments in which the light particles are recorded together with the velocity of the residue will be of great value.

This work was supported by the Director, U.S. Office of Energy Research, Division of Nuclear Physics of the Office of High Energy and Nuclear Physics, and by Nuclear Sciences of the Basic Energy Sciences Program of the U. S. Department of Energy under Contract No. DE-AC03-76SF00098.

References:

1) K. Siwek-Wilczynska, E. H. du Marchie van Voorthuysen, J. van Popta, R. H. Siemssen, and J. Wilczynski, Phys. Rev. Lett., 42 1599 (1979), Nucl. Phys. A330, 150 (1979).

2) T. Inamura, M. Ishihara, T. Fukuda, and T. Shimoda, Phys. Lett., 69B, 51 (1977).

D. R. Zolnowski, H. Yamada, S. E. Cala, A. C. Kahler, and T. T. Sugihara, Phys. Rev. Lett., 41, 92 (1978).

3) J. J. Griffin, Phys. Rev. Lett., 17, 478 (1966).

M. Blann, Ann. Rev. Nucl. Sci., 25, 123 (1975).

4) S. E. Vigdor, D. G. Kovar, P. Sperr, J. Mahoney, A. Menchaca-Rocha, C. Olmer, and M. S. Zisman, Phys. Rev. C20, 2147 (1979).

5) H. Ho, P. Gonthier, M. N. Namboodiri, J. B. Natowitz, L. Adler, S. Simon, K. Hagel, R. Terry, and A. Khodai, Phys. Lett. 96B, 51 (1980).

6) P. Gonthier, H. Ho, M. N. Namboodiri, L. Adler, J. B. Natowitz, S. Simon, K. Hagel, R. Terry, and A. Khodai, Phys. Rev. Lett., 44, 1387 (1980).

7) B. B. Back, K. L. Wolf, A. C. Mignerey, C. K. Gelbke, T. C. Awes, H. Breuer, V. E. Viola, Jr., and P. Dyer, Phys. Rev. C22, 1927 (1980).

8) J. Gomez del Campo, R. G. Stokstad, J. A. Biggerstaff, R. A. Dayras, A. H. Snell, and P. H. Stelson, Phys. Rev. C19, 2170 (1979).

9) LILITA, A Monte Carlo Hauser-Feshbach Code. J. Gomez del Campo and R. G. Stokstad, ORNL TM-7295, Oak Ridge National Laboratory.

10) V. Viola, Jr., B. B. Back, K. L. Wolf, T. C. Awes, C. K. Gelbke, and H. Breuer, Phys. Rev. C26, 178 (1982).

11) H. Morgenstern, W. Bohne, K. Brabish, D. G. Kovar, and H. Lehr, Phys. Lett., 113B, 463 (1982).

12) E. Duek, L. Kowalski, M. Rajagopalan, J. M. Alexander, D. Logan, M. S. Zisman and M. Kaplan, Z. Phys. A 307, 221 (1982).

13) T. Udagawa and T. Tamura, Phys. Rev. Lett. 45, 1311 (1980).

14) W. J. Nickolson and I. Halpern, Phys. Rev. 116, 175 (1958)

15) S. S. Kapoor, H. Baba, and S. G. Thomspon, Phys. Rev. 149, 965 (1966).

16) J. Galin, H. Oeschler, S. Song, B. Borderie, M. F. Rivet, I. Forest, R. Bimbot, D. Gardes, B. Gatty, H. Guillemot, M. Lefort, B. Tamain, and X. Tarrago, Phys. Rev. Lett. 46, 1787 (1982).

17) V. E. Viola, R. G. Clark, W. G. Meyer, A. M. Zebelman and R. G. Sextro, Nucl. Phys. A261, 174 (1976).

18) T. Sikkeland, E. L. Haines, and V. E. Viola, Jr., Phys. Rev. 125 1350 (1962). T. Sikkeland and V.E. Viola, Proc. Second Int. Conf. on Heavy Ion Reactions, Asilomar (1964).

Table I. List of reactions included in Fig. 13.

Symbol	Proj+target	E/A_p	$((E-V_c)/A_p)^{1/2}$	P_{res}/P_{beam}	Ref.
a	$^{12}C + ^{238}U$	6.2	0.94	100±3	10
b	$^{16}O + ^{238}U$	6.9	1.28	99±3	14,10
c	$^{12}C + ^{238}U$	7.8	1.57	101±3	10
d	$^{16}O + ^{238}U$	8.8	1.87	101±3	18
e	$^{20}Ne + ^{235}U$	8.8	1.87	97±2	15,10
f	$^{20}Ne + ^{235}U$	8.8	1.87	95±1	12
g	$^{12}C + ^{238}U$	10.4	2.25	98±3	14,10
h	$^{20}Ne + ^{238}U$	10.4	2.27	96±3	10
i	$^{16}O + ^{238}U$	10.4	2.27	97±1	12
j	$^{12}C + ^{238}U$	10.4	2.27	96±1	12
k	$^{12}C + ^{197}Au$	10.4	2.36	100±3	18,16
l	$^{16}O + ^{197}Au$	10.4	2.37	99±1	12
m	$^{20}Ne + ^{197}Au$	10.4	2.37	95±1	12
n	$^{16}O + ^{165}Ho$	10.4	2.47	99±1	12
o	$^{16}O + ^{40}Ca$	8.8	2.56	94±4	present work
p	$^{16}O + ^{27}Al$	8.8	2.65	97±4	present work
q	$^{20}Ne + ^{235}U$	12.5	2.70	93±2	17
r	$^{16}O + ^{60}Ni$	13.6	3.31	92±4	present work
s	$^{16}O + ^{40}Ca$	13.6	3.37	88±4	present work
t	$^{16}O + ^{27}Al$	13.6	3.44	91±4	present work
u	$^{20}Ne + ^{40}Ca$	14.6	3.50	89±5	11
v	$^{16}O + ^{238}U$	19.7	3.80	92±4	7
w	$^{16}O + ^{60}Ni$	19.6	4.12	81±4	present work
x	$^{16}O + ^{40}Ca$	19.6	4.17	79±4	present work
y	$^{16}O + ^{27}Al$	19.6	4.22	83±4	present work
z	$^{12}C + ^{197}Au$	30.0	5.02	67±7	16

Figure Captions:

1) A schematic diagram of the time-of-flight apparatus used to measure the velocity of the fusion residues.

2) The calibration of the velocity scale by measurement of elastic scattering of oxygen and argon beams from various targets.

3) A two-dimensional spectrum of mass versus energy. Note the intense yield of mass numbers from 35-47. This shows the clean separation of the evaporation residue component from other reaction meachanisms.

4) A projection of the results in Fig. 3 onto the mass axis.

5) The velocity spectrum for mass 43 at 5°. The shape of the spectrum is well approximated by a Gaussian.

6) Velocity spectra for different masses observed at 15°. The bombarding energy is 8.8 MeV/nucleon.

7) Velocity spectra for different masses observed at 5°. The bombarding energy is 13.6 MeV/nucleon.

8) A comparison of the measured centroids with $v_{c.m.}\cos\theta$ for different masses observed at 5° to 25°. The relative intensity of each mass is indicated by the histogram. The bombarding energy is 8.8 MeV/nucleon.

9) A comparison of the measured centroids with $v_{c.m.}\cos\theta$ for different masses observed at 5° to 20°. The relative intensity of each mass is indicated by the histogram. The bombarding energy is 13.6 MeV/nucleon.

10) A comparison of the measured centroids with $v_{c.m.}\cos\theta$ for different masses observed at 5° and 12°. The relative intensity of each mass is indicated by the histogram. The bombarding energy is 19.6 MeV/nucleon.

11) Comparison of $\overline{v}/\cos\theta$ of the reduced velocity spectra (see text) with the center-of-mass velocity at (a) 8.8 MeV/nucleon, (b) 13.8 MeV/nucleon, and (c) 19.6 MeV/nucleon. The relative mass yields at 5° are shown by histograms.

12) Systematics of the mean velocities of fusion-like residues, expressed as a percentage of the velocity corresponding to complete momentum transfer. The abscissa is the relative velocity of the projectile and target at the interaction barrier (using r_o = 1.5 fm). The energy E and Coulomb barrier V_c are evaluated in the laboratory system. The results from Ref. 7 were obtained using the fission-fragment angular-correlation technique.

13) Systematics of the mean velocities of fusion-like residues, as above, and including data for ^{12}C and ^{20}Ne beams. A listing of the reactions and the references is given in Table I.

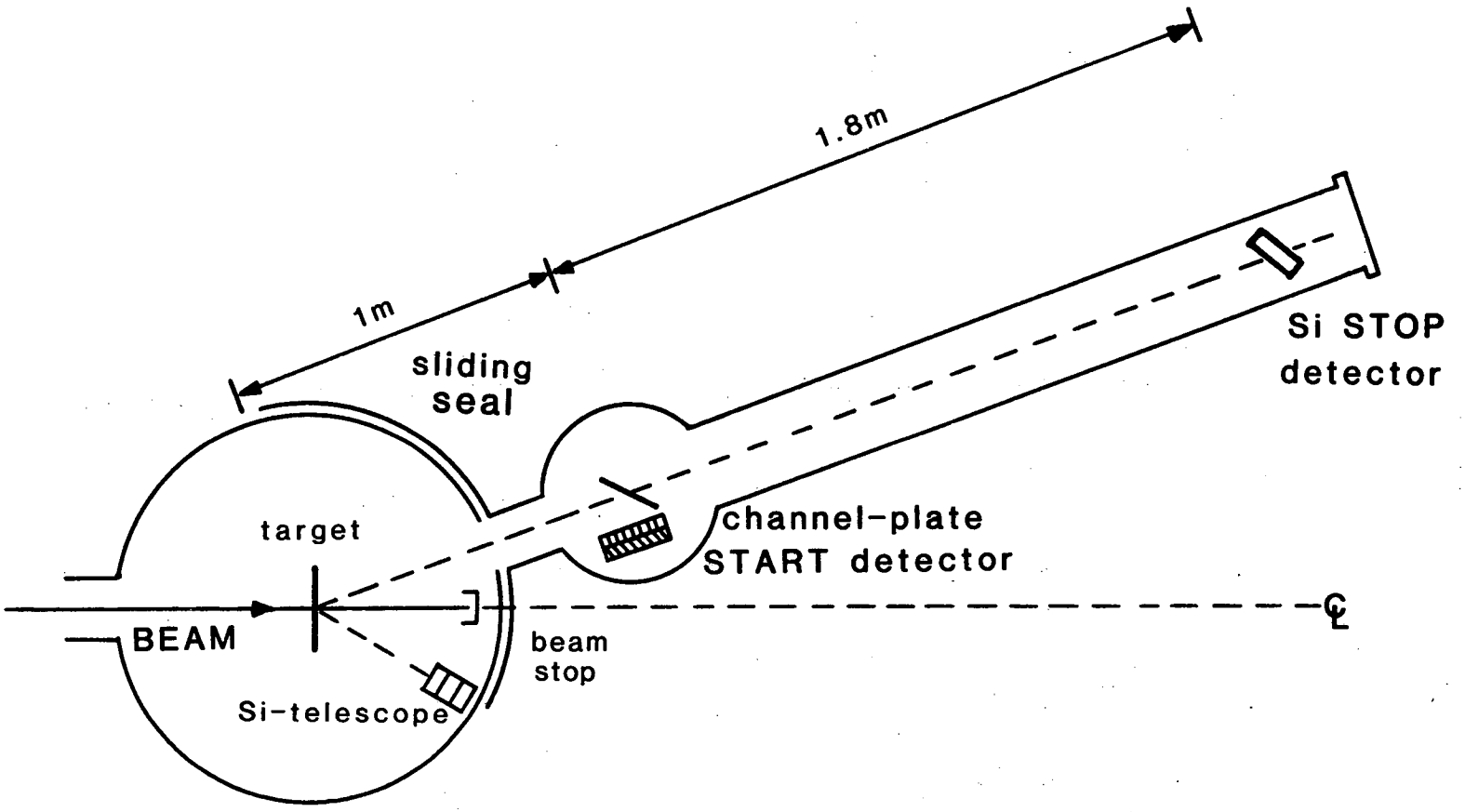

T.O.F. Experiment Schematic Drawing

XBL 8212-12423

Fig. 1

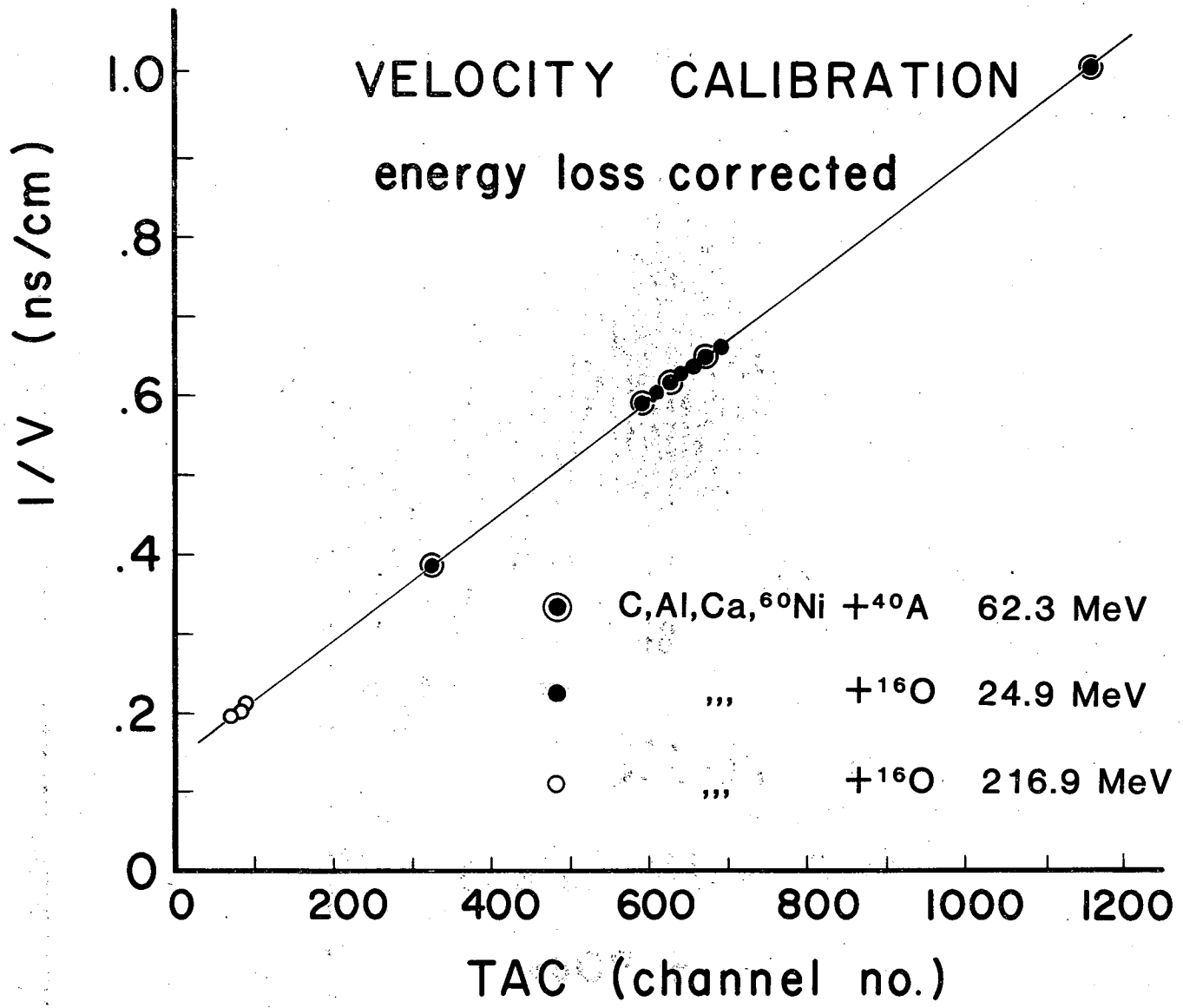

XBL 8212-12428

Fig. 2

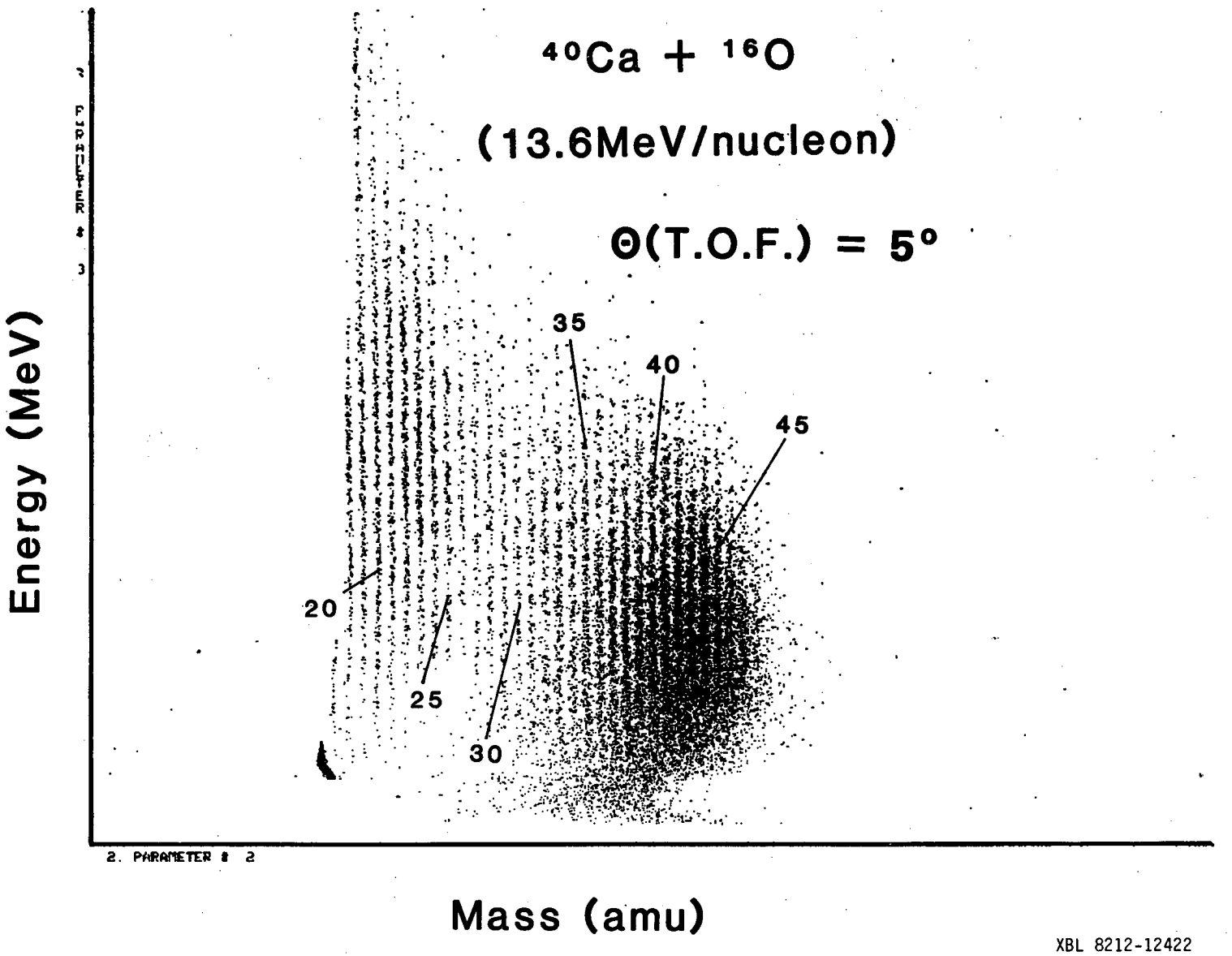

XBL 8212-12422

Fig. 3

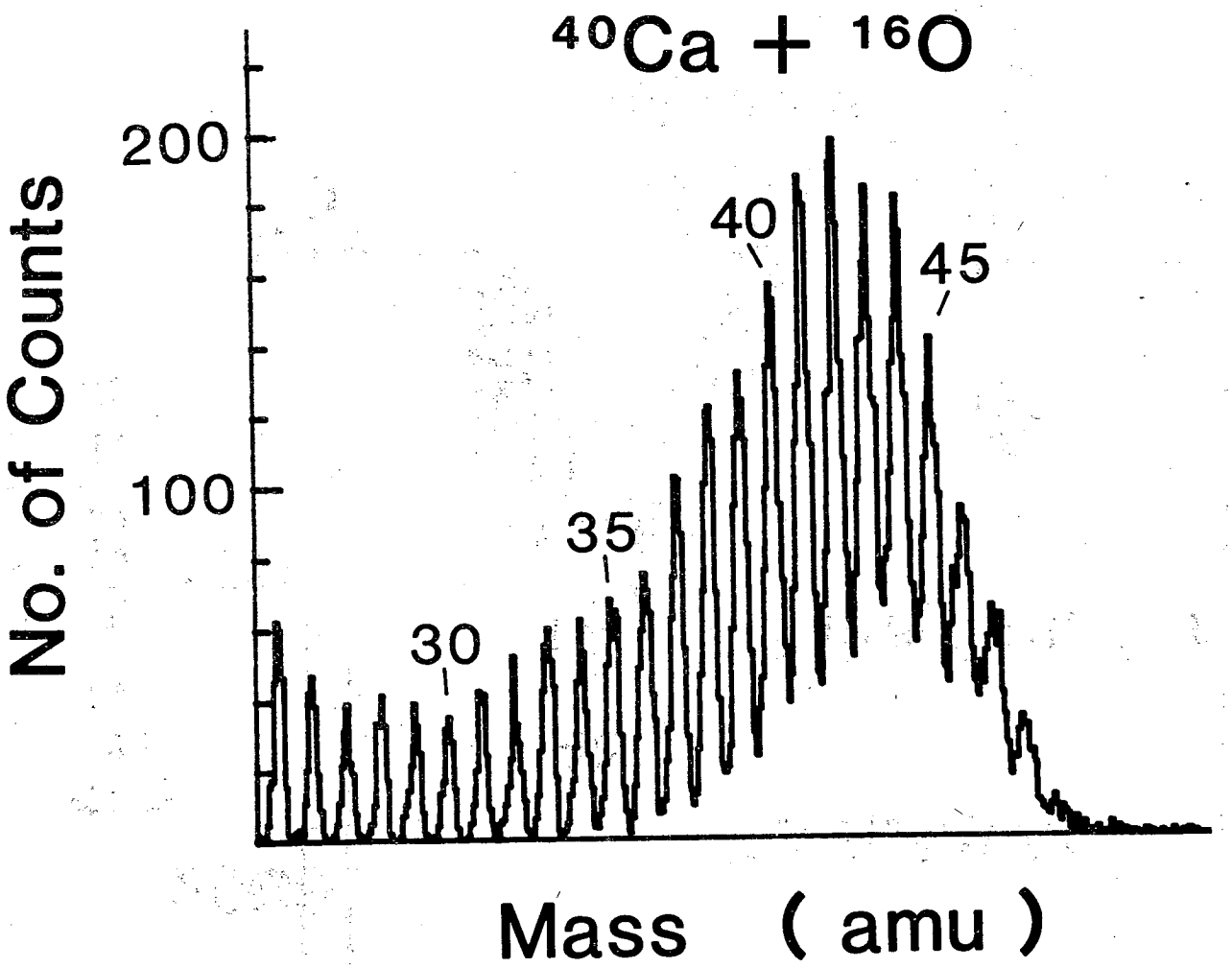

Fig. 4 XBL 8212-12426

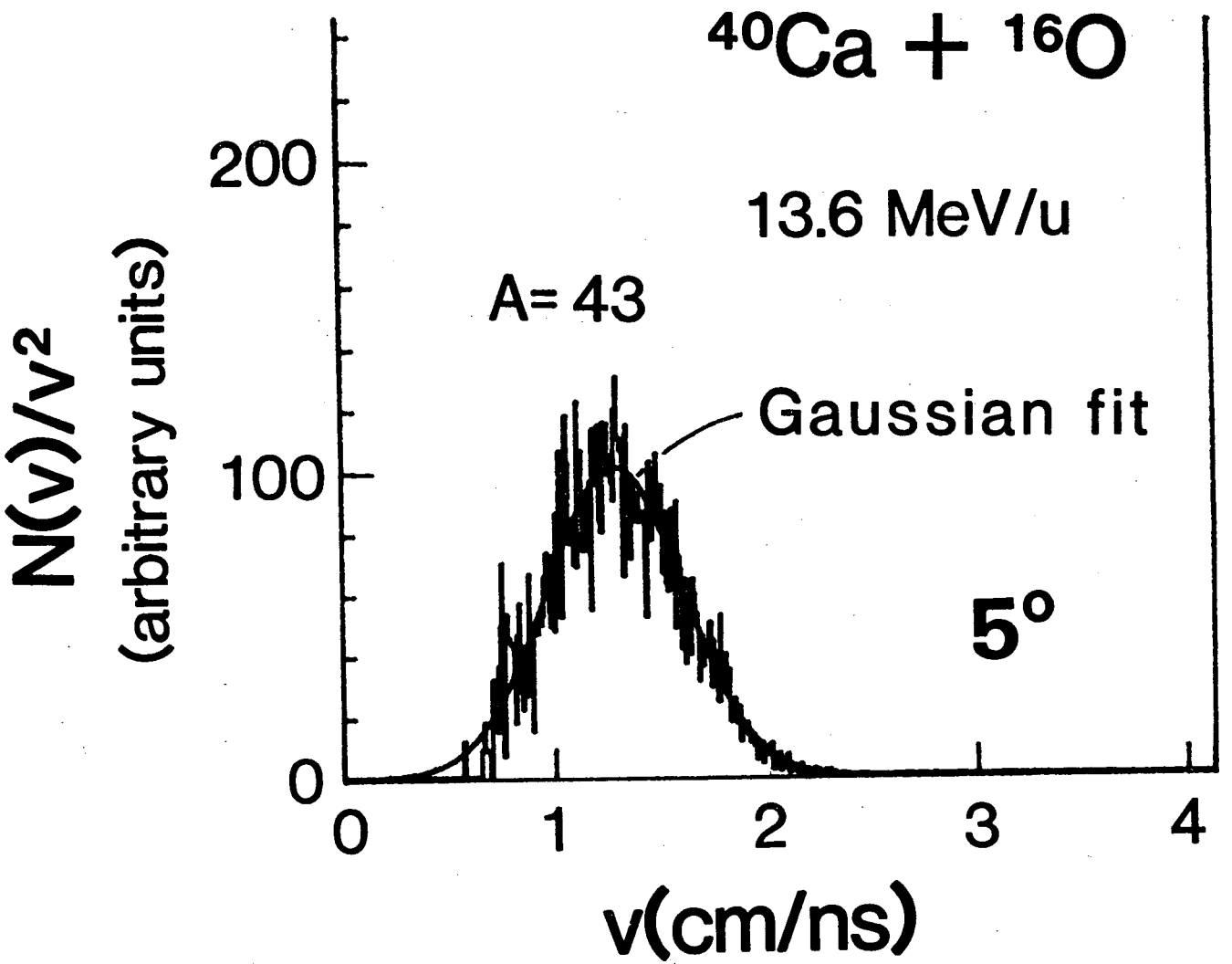

XBL 8212-12427

Fig. 5

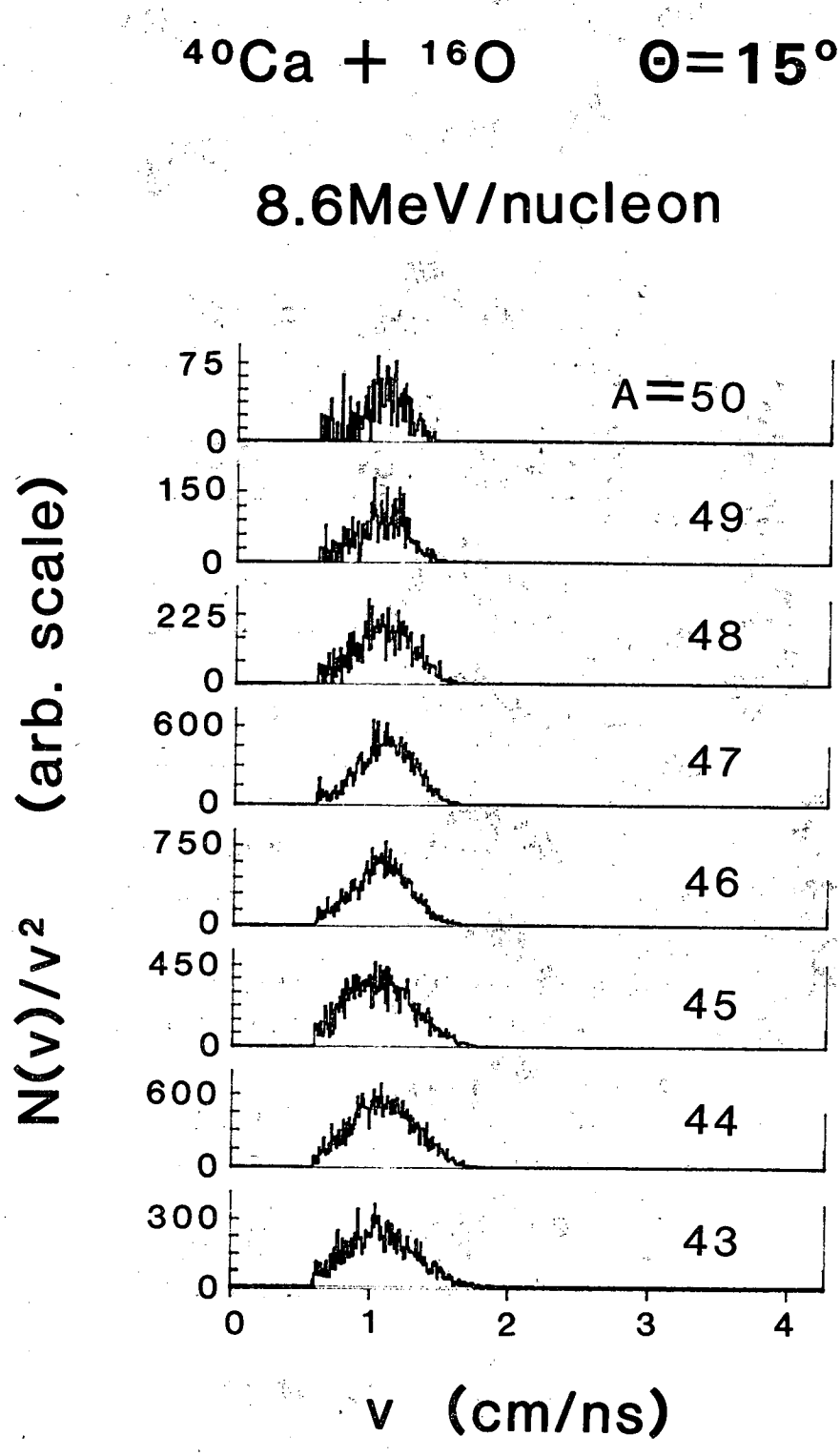

XBL 8212-12424

Fig. 6

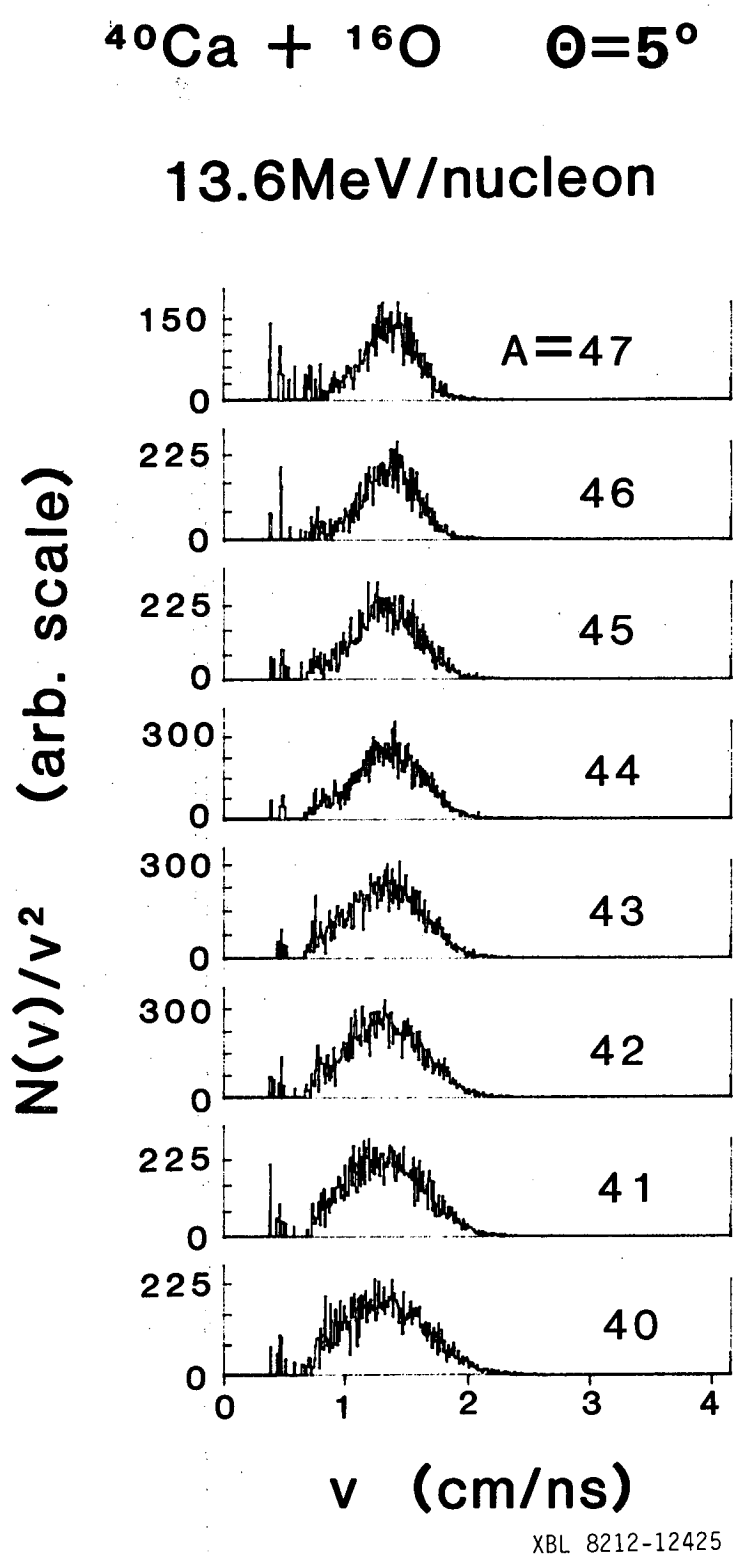
$^{40}Ca + ^{16}O$ $\Theta=5°$
13.6MeV/nucleon
N(v)/v² (arb. scale)
150
0
A=47
225
0
46
225
0
45
300
0
44
300
0
43
300
0
42
225
0
41
225
0
40
0
1
2
3
4
v (cm/ns)
XBL 8212-12425

Fig. 7

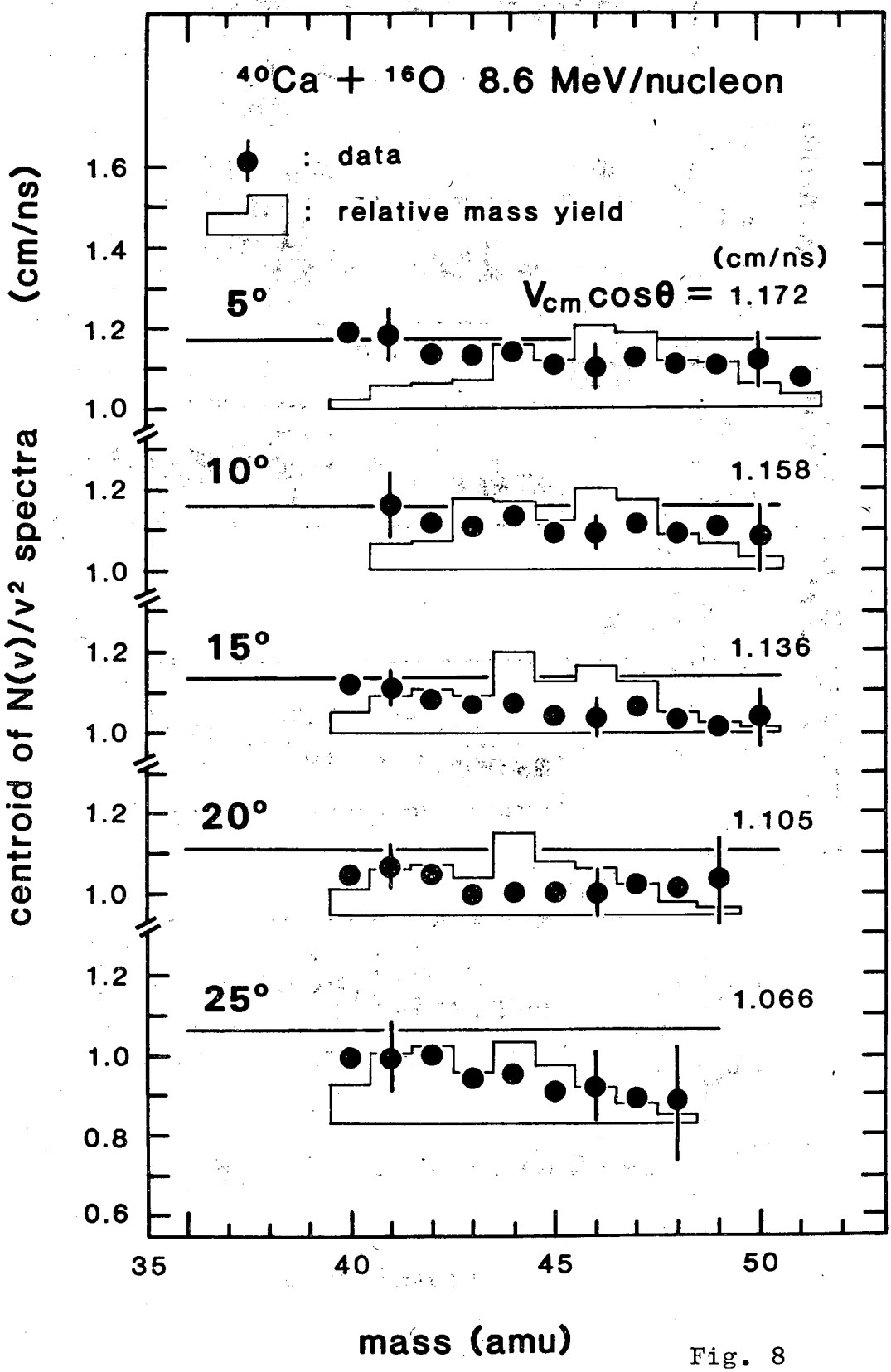
^{40}Ca + ^{16}O 8.6 MeV/nucleon
: data
: relative mass yield
(cm/ns)
$V_{cm}\cos\theta$ = 1.172
5°
10°
1.158
15°
1.136
20°
1.105
25°
1.066
centroid of N(v)/v² spectra (cm/ns)
mass (amu)
1.6
1.4
1.2
1.0
0.8
0.6
35
40
45
50

Fig. 8

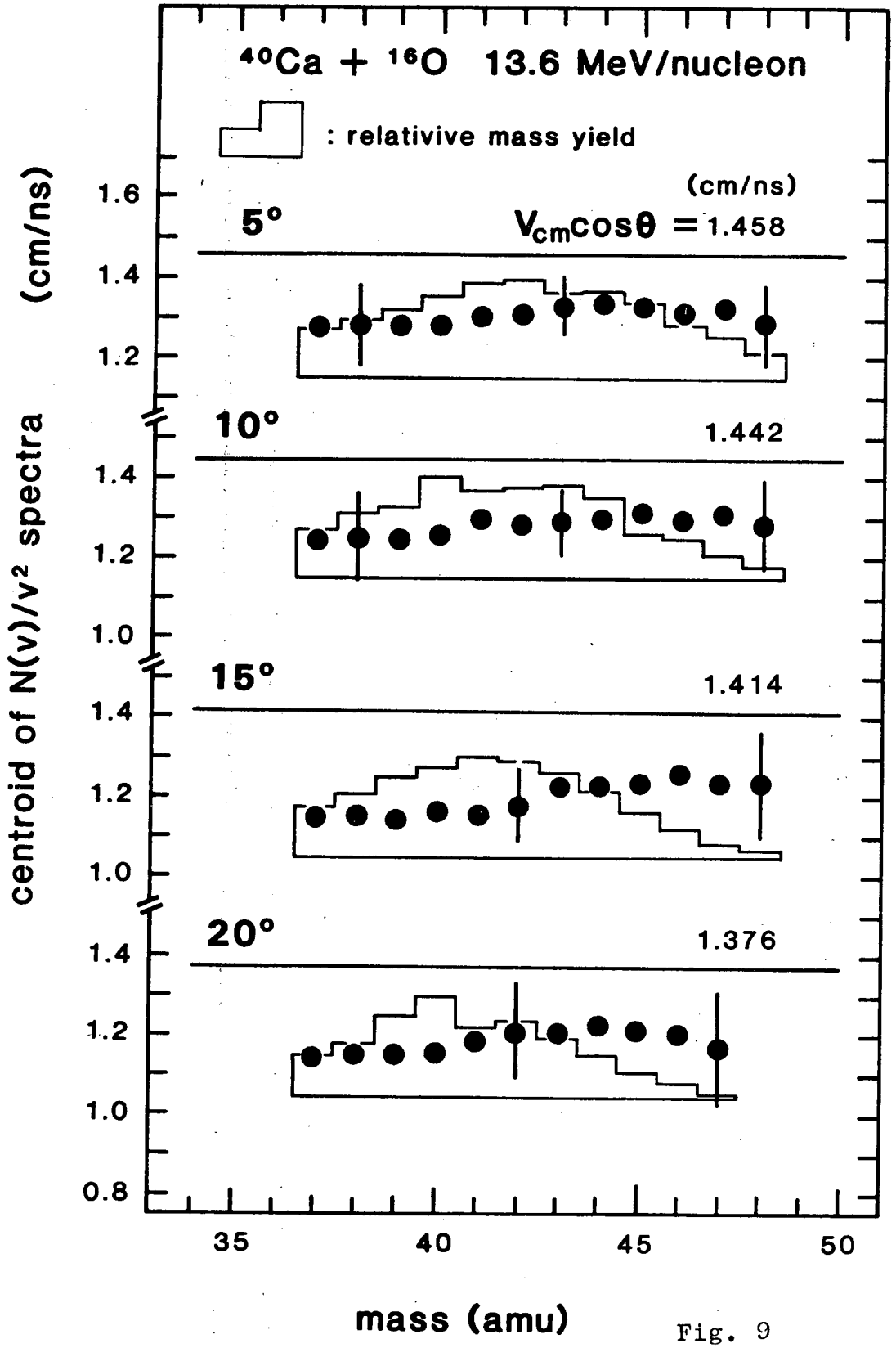
^{40}Ca + ^{16}O 13.6 MeV/nucleon
: relativive mass yield
(cm/ns)
$V_{cm}\cos\theta$ = 1.458
5°
1.442
10°
1.414
15°
1.376
20°
centroid of N(v)/v² spectra (cm/ns)
mass (amu)
35
40
45
50
0.8
1.0
1.2
1.4
1.6

Fig. 9

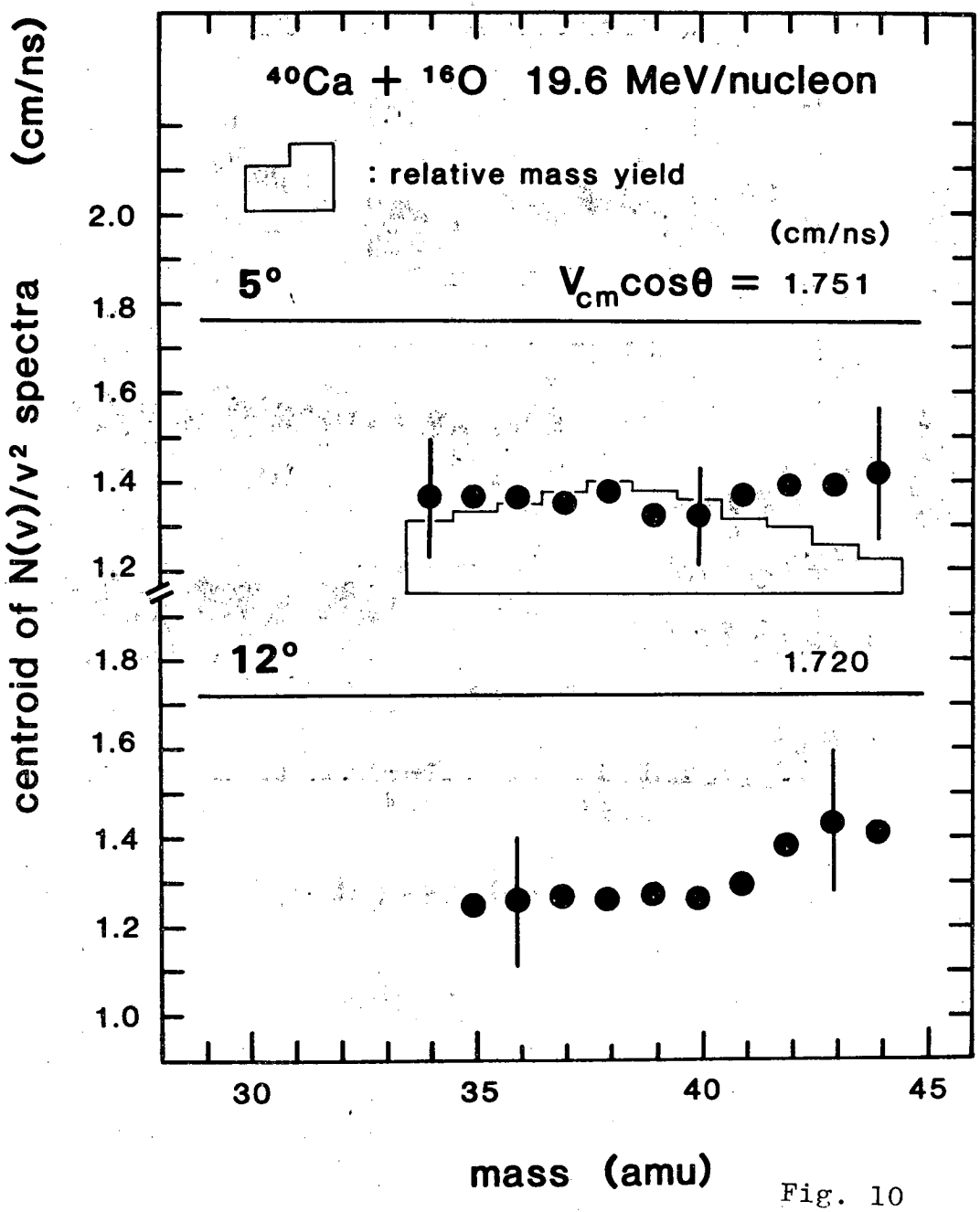
^{40}Ca + ^{16}O 19.6 MeV/nucleon
: relative mass yield
(cm/ns)
5°
$V_{cm}\cos\theta$ = 1.751
12°
1.720
centroid of N(v)/v² spectra (cm/ns)
2.0
1.8
1.6
1.4
1.2
1.8
1.6
1.4
1.2
1.0
30
35
40
45
mass (amu)

Fig. 10

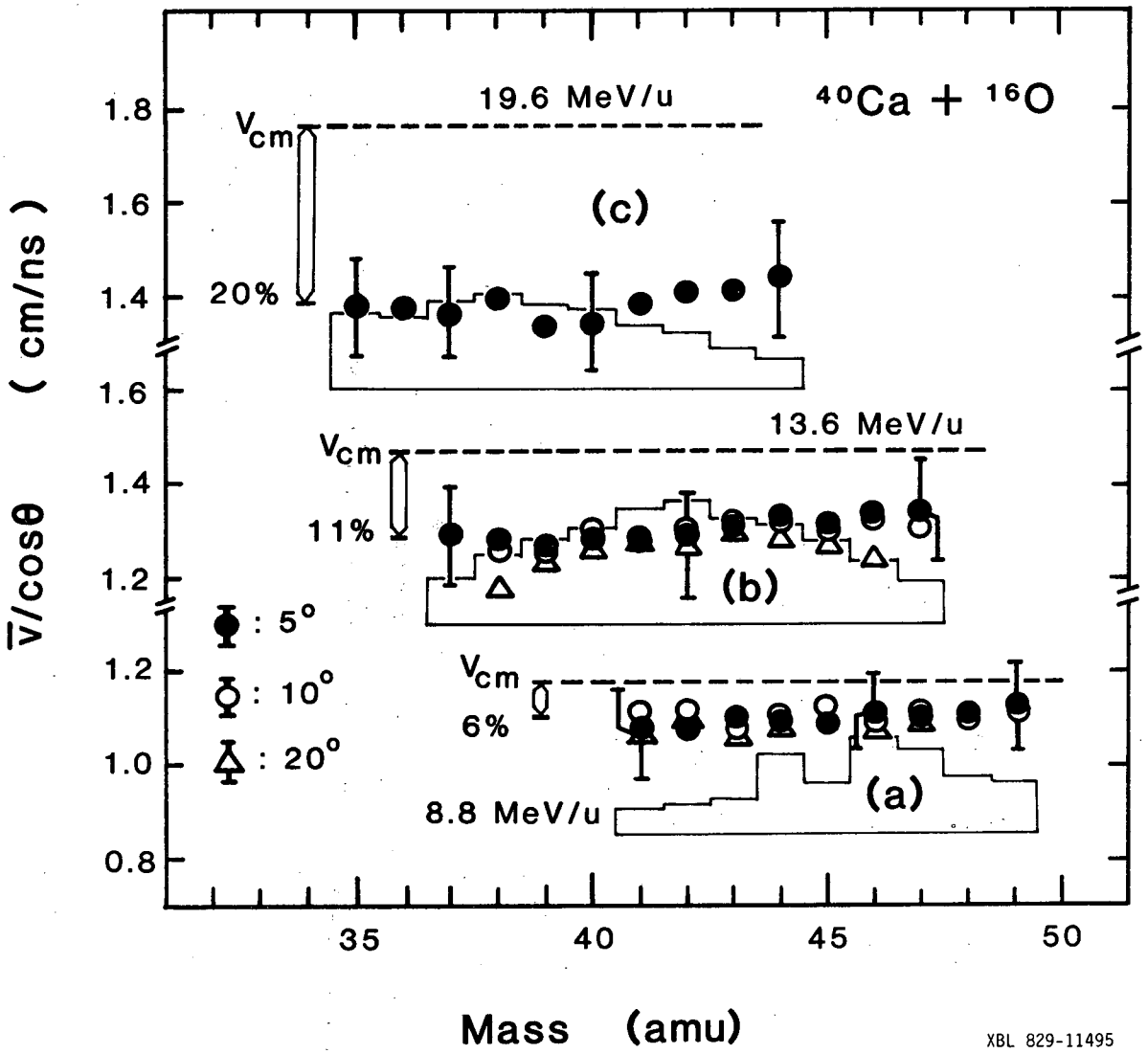
19.6 MeV/u
^{40}Ca + ^{16}O
V_{cm}
(c)
20%
13.6 MeV/u
V_{cm}
11%
(b)
: 5°
: 10°
: 20°
V_{cm}
6%
(a)
8.8 MeV/u
$\bar{v}/\cos\theta$ (cm/ns)
Mass (amu)
XBL 829-11495

Fig. 11

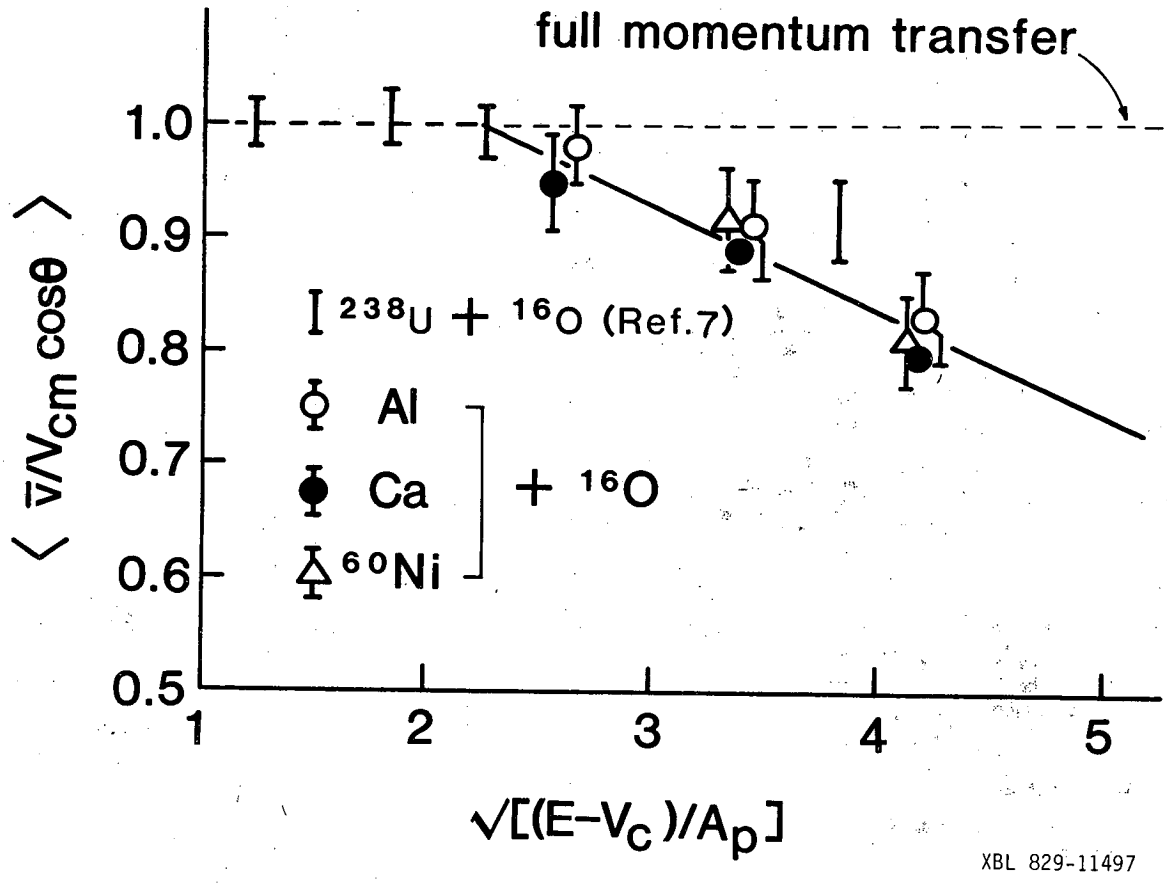
full momentum transfer
1.0
0.9
0.8
0.7
0.6
0.5
1
2
3
4
5
$\langle \bar{v}/V_{cm} \cos\theta \rangle$
$\sqrt{[(E-V_c)/A_p]}$
$^{238}U + ^{16}O$ (Ref.7)
Al
Ca
^{60}Ni
$+ ^{16}O$
XBL 829-11497

Fig. 12

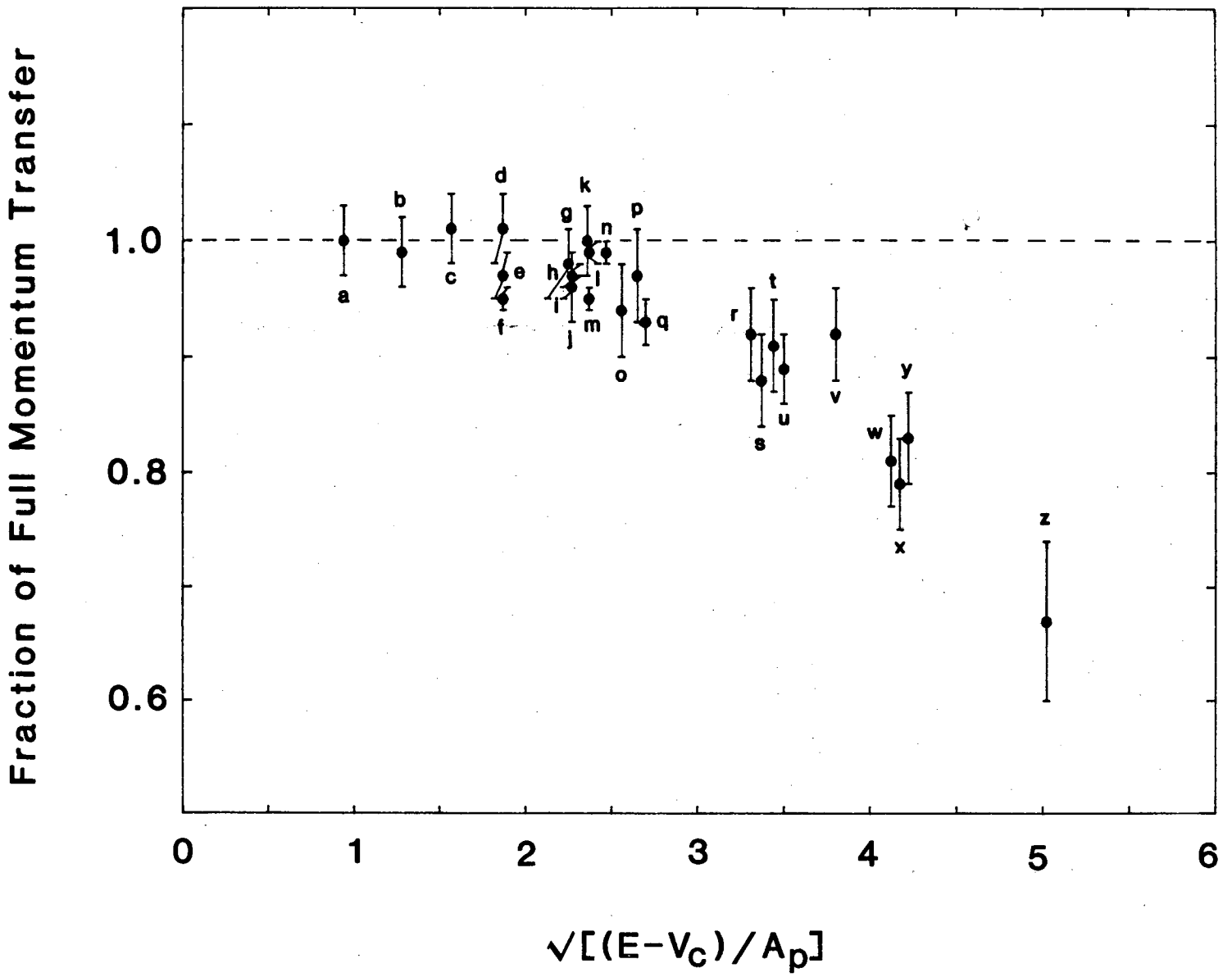
Fraction of Full Momentum Transfer
1.0
0.8
0.6
0
1
2
3
4
5
6
√[(E−Vc)/Ap]
a
b
c
d
e
f
g
h
i
j
k
l
m
n
o
p
q
r
s
t
u
v
w
x
y
z

Fig. 13

This report was done with support from the Department of Energy. Any conclusions or opinions expressed in this report represent solely those of the author(s) and not necessarily those of The Regents of the University of California, the Lawrence Berkeley Laboratory or the Department of Energy.

Reference to a company or product name does not imply approval or recommendation of the product by the University of California or the U.S. Department of Energy to the exclusion of others that may be suitable.

TECHNICAL INFORMATION DEPARTMENT
LAWRENCE BERKELEY LABORATORY
UNIVERSITY OF CALIFORNIA
BERKELEY, CALIFORNIA 94720